Chlorine residue in the Au/γ-Al_2O_3 prepared by $AuCl_3$ impregnation—an EXAFS analysis

Chih-Hui Lin[a], Shawn D. Lin[a,*], and Jyh-Fu Lee[b]

[a]*Department of Chemical Engineering, Yuan Ze University, Chung-Li, Taoyuan 320, Taiwan, R.O.C.*
[b]*National Synchrotron Radiation Research Center, Hsinchu 300, Taiwan, R.O.C.*

Received 8 May 2003; accepted 11 June 2003

From EXAFS (extended X-ray absorption fine structure) analysis, gold was found to have mainly oxygen in its nearest coordination shell in the fresh Au/γ-Al_2O_3 catalyst prepared by $AuCl_3$ impregnation and vacuum drying at room temperature. After thermal treatment under helium, chlorine appeared within the nearest neighbors of gold and more chlorine showed up as the treatment temperature was increased from 323 to 473 K. No reduced Au species was observed up to 473 K under He. However, the gold became reduced during CO oxidation at 373 K and above. The precursor $AuCl_3$ was found to deposit on γ-Al_2O_3 via bonding to surface hydroxyl groups. This catalyst showed nearly 100% CO conversion at 573 K, but a very low activity at $\leq$373 K under the conditions used in this study. Neither the residual chlorine nor the extent of reduction can explain the low activity at lower temperatures.

KEY WORDS: residual chlorine; gold; γ-Al_2O_3; *in situ* EXAFS.

1. Introduction

Supported gold catalysts were found to catalyze CO oxidation readily even at a temperature as low as 200 K [1]. However, such a high activity can be obtained mainly with catalysts having nanosized Au particles and in the absence of chlorine residue [2]. Coprecipitation and deposition were both considered applicable preparation methods when thorough washing was implemented to remove chlorine residue [3]. Chemical vapor deposition was also reported effective [4] but only very few chlorine-free volatile precursors are commercially available. Incipient-wetness impregnation was mostly concluded as an ineffective preparation method for gold catalysts based on activity analyses [5]. This is typically attributed to the chlorine residue or gold particle size or both, although no direct proof was provided. Oh *et al.* [6] recently reported that the presence of Cl residue caused Au agglomeration during heat treatment and activity suppression. However, their catalyst preparation adopted the deposition method, and the status of surface Cl might be affected by pH adjustment, washing, or the addition of magnesium citrate. This study is intended to get an insight on how residual chlorine affects the performance of gold catalysts, by studying the catalyst prepared by $AuCl_3$ impregnation. The EXAFS (extended X-ray absorption fine structure) spectroscopy is utilized as the main characterization tool. The morphology as prepared, that after thermal treatment, and that under reaction conditions, will be reported. Although different oxide supports were reported effective to give active Au catalysts, the metal-support interaction is considered as one important reason for the high activity [7]. In order to exclude the possible effect of metal-support interaction, we choose γ-Al_2O_3, a refractory oxide, as the support for our gold catalysts.

2. Experimental

Au/γ-Al_2O_3 catalyst of 1 wt% Au loading was prepared by impregnating γ-Al_2O_3 support (Strem, 99$^+$ %, low soda, 220 m^2/g, 80–120 mesh, precalcined at 823 K for 1 h) with $AuCl_3$ (Aldrich, 64.9% Au) aqueous solution to incipient wetness and then dried at 298 K under low vacuum. TEM analysis showed that the majority of Au particles were below 5 nm with only a few particles of around 5–10 nm.

CO oxidation was performed with a feed of 1% CO + 10% O_2 (balanced with He) in a flow-type packed-bed reactor operated at 1 atm. Before measurement, the Au catalyst was purged inline with He at room temperature for 30 min and then pretreated, if needed, followed by cooling under He atmosphere. The reactant mixture was admitted after the reactor reached the preset reaction temperature. The CO space velocity was kept at 71.4 μmol/min/g catalyst. Typically, the reaction test was performed according to a stepwise temperature-ascending–descending sequence with He purge during the course of temperature changes. The reactor effluent was analyzed using a GC (China

* To whom correspondence should be addressed.
E-mail: sdlin@saturn.yzu.edu.tw

1011-372X/03/0900–0235/0

Chromatography 8900) in line via a 6-port valve (Valco), with an active carbon-packed column and a thermal conductivity detector. The CO conversion is defined as the amount of CO_2 divided by the total amount of $CO + CO_2$ of the effluent. The carbon balance at effluent was typically within ±10% of the inlet stream. Usually, the conversion at each temperature became stable after 30 min on stream and the recorded conversion was that after 1 h on stream.

EXAFS experiments were performed on the wiggler beam line (BL17C) at the National Synchrotron Radiation Research Center, Taiwan, with a storage ring energy of 1.5 GeV and a beam current between 120 and 200 mA. The Au L_{III}-edge absorbance of powder catalysts was measured in transmission geometry, typically at 298 K unless otherwise specified. The energy was scanned from −200 to +1200 eV, relative to the Au L_{III}-edge (11919 eV). EXAFS data analysis was carried out using the UWXAFS package [8]. Radial distribution function was obtained by a Fourier transformation of k^3-weighted χ function. Detailed analysis was carried out by fitting the EXAFS data in a k-range from 3 to 13 $Å^{-1}$. A k^3-weighting was used for all the analysis for emphasizing the possible contribution from second shells. Comparison made with lower k-weighting did not reveal a significant difference in the first shell coordination. This fitting was performed against selected combinations from the following coordination shells: Au–O, Au–Cl, Au · · · · Al, Au–Au, and Au–Au2. All these reference shells are obtained by theoretical calculations from specific atom pairs using the code Feff 7.02 [9]. The Au-O shell has a bond distance of 2.04 Å [10], consistent with the average of Au–Au (2.88 Å) and O–O (1.20 Å). The Au–Cl shell with a bond distance of 2.28 Å [11] is used, slightly shorter than the average of Au–Au (2.88 Å) and Cl–Cl (1.99 Å). The Au · · · · Al shell is initiated to identify adsorbed Au species via surface hydroxyl groups. The bond distance of Au · · · · Al is assumed as 3.4 Å, slightly shorter than the sum of Au–O (2.04 Å) and O–Al (1.62 Å) to take the bond angle into consideration. The Au–Au2 stands for the second shell metallic binding in an Au fcc cuboctahedral crystal. For *in situ* EXAFS experiments, the catalyst powders were pressed into a self-supporting wafer and mounted on the sample holder inside a control-atmosphere chamber. The *in situ* cell was made following the design concept of Kampers *et al.* [12]. Reference compounds, $AuCl_3$ (Aldrich) and $Au(OH)_3$ (Aldrich), were measured *ex situ* by spreading powders over tapes.

In situ diffuse-reflectance UV-visible spectroscopy (DRS) was also carried out in the same manner as the *in situ* EXAFS experiment under He purging at different temperatures. A commercial unit (Hitachi, 3410) equipped with a 60 φ integrating sphere was used. Barium sulfate was used as the reference and the scan was from 800 to 200 nm at 10 nm/min with a band pass of 2 nm. A house-made cell was used to treat and measure the sample under controlled atmosphere.

3. Results

The effect of thermal treatment on the fresh impregnated sample was studied with *in situ* EXAFS. The fresh sample was measured first, then purged overnight with dry He at 298 K, and then treated in a stepwise temperature-ascending sequence under He. Figure 1 shows the radial distribution functions recorded at 298 K after each treatment; phase correction was not implemented in figure 1. Surprisingly, the fresh sample contained mainly a Au–O coordination shell with no evidence for Au–Cl. This indicates that the Au deposit was formed with chlorine ligands replaced by, most likely, −OH ligands. However, the Au–Cl coordination shell appeared after the fresh sample was further dried by overnight helium purge and the Au–Cl contribution became more and more significant with increasing treatment temperature. This suggests that chlorine residue in the as-prepared sample was either located near the Au deposit but not directly bonded to Au or incorporated into the support. Treating at elevated temperatures led to a reduced density of hydroxyl groups, causing chlorine to bond to Au again.

Table 1 lists the results of detailed EXAFS analysis. The goodness of fitting can be found in figures 1 and 2. In addition to the Au–O coordination, the fresh sample contained an Au · · · · Al coordination shell at ca. 3.5 Å, slightly shorter than the sum of Au–O and Al–O. This suggests a bonding configuration as Au–O–Al, and that hydroxyl groups on Al_2O_3 acted as anchors to Au deposit. The presence of Au–O–Al coordination is consistent with the reported uptake of Au (III) ions by aluminum hydroxide [13] and the proposed Au hydroxochloride complex adsorption on γ-Al_2O_3 [14,15]. The Au–O coordination number decreased when the sample was treated with increasing temperature. Instead of Au–O, the Au–Cl coordination increased while the sum of Au–O and Au–Cl coordination numbers maintained at

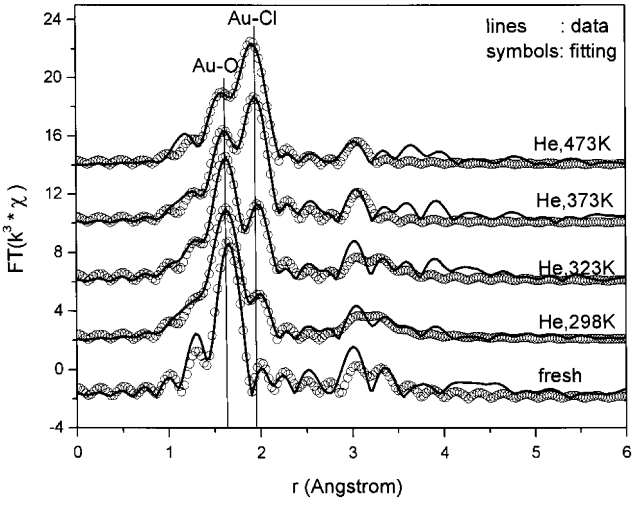

Figure 1. Effect of thermal treatment on the radial distribution function of the Au/γ-Al_2O_3 prepared by impregnation.

Table 1
EXAFS analysis results of thermal-treated Au/γ-Al_2O_3 prepared from $AuCl_3$ impregnation

Sample	Shell	r (Å)	C.N.	σ^2	E_0 (eV)	r-factor
Fresh	Au–O	1.995±0.009	2.8±0.6	0.002±0.001	8.8±2.3	0.063
	Au–Cl	2.260±0.014	0.01±0.04	−0.009±0.009		
	Au····Al	3.498±0.044	5.7±4.5	0.014±0.011		
He purge, 298 K, overnight	Au–O	1.981±0.010	2.9±0.6	0.003±0.001	6.6±1.3	0.027
	Au–Cl	2.251±0.016	0.6±0.5	0.003±0.004		
	Au····Al	3.500±0.023	6.0±2.3	0.018±0.006		
He purge, 323 K, 30 min	Au–O	1.989±0.014	2.6±0.8	0.002±0.002	7.6±1.6	0.060
	Au–Cl	2.263±0.012	0.7±0.5	0.001±0.003		
	Au····Al	3.506±0.035	6.2±4.0	0.020±0.010		
He purge, 373 K, 30 min	Au–O	1.986±0.025	1.5±0.9	0.002±0.003	6.0±1.8	0.046
	Au–Cl	2.260±0.011	1.7±0.7	0.003±0.002		
	Au····Al	3.389±0.016	0.5±0.4	−0.001±0.003		
He purge, 473 K, 30 min	Au–O	1.973±0.033	1.0±0.8	0.002±0.004	4.2±1.7	0.042
	Au–Cl	2.254±0.010	2.1±0.7	0.004±0.002		
	Au····Al	3.372±0.019	0.5±0.4	0.0004±0.003		

around 3.0–3.5. This indicates that the Au deposit was not reduced by thermal treatment up to 473 K. The surface Au species may assume oxychloride-like morphology. However, the Au····Al coordination shell was mostly removed after being treated at 373 K and above. This suggests that the reformed Au–Cl bonding is not bridged to Al_2O_3 surface. This provides an explanation why the presence of Cl residue resulted in Au agglomeration during heat treatment as reported earlier [6].

Figure 3 shows the corresponding XANES (X-ray absorption near-edge structure) spectra. The Au–O morphology dominated in the fresh sample showed a higher white line and the presence of a +25 eV (above white line) broad resonance feature. On the other hand, a +12 eV resonance feature and a lower white line were found with the Au–Cl morphology that appeared after the sample was treated at above 373 K. As compared with the reference compounds, it seems reasonable to attribute the +12 eV resonance to the presence of Cl-ligand of Au centers. A similar shift from +12 to +25 eV resonance was also observed in the Au/γ-Al_2O_3 prepared by a deposition method [16] and in $Au(OH)_xCl_{y(aq)}$ [17] when the pH was increased.

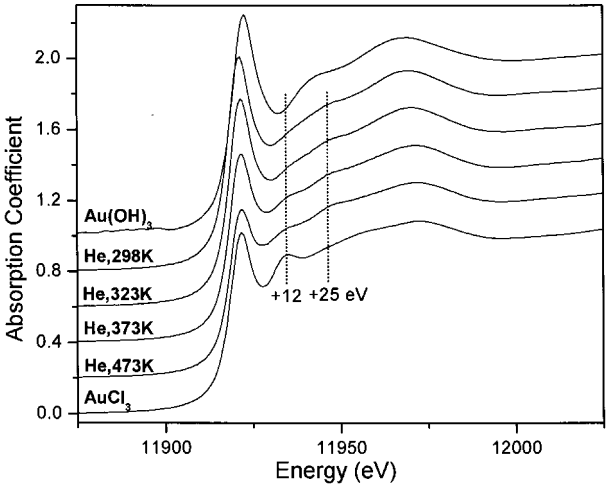

Figure 3. Effect of thermal treatment on the near-edge X-ray absorption of the Au/γ-Al_2O_3 prepared by $AuCl_3$ impregnation.

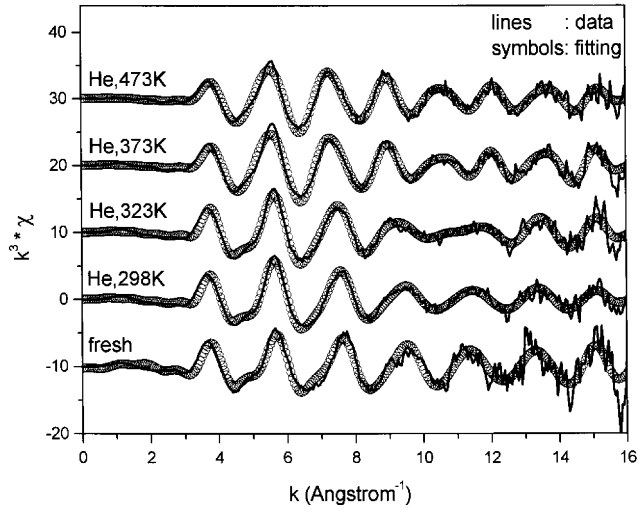

Figure 2. Effect of thermal treatment on the k^3-weighted Chi function of the Au/γ-Al_2O_3 prepared by impregnation.

Results of *in situ* DRS measurements following identical thermal treatment procedures can be found in figure 4. The most prominent absorption peak appears at 214 nm and some less-intense peaks can be found at 254, 283, and 310 nm respectively. No surface plasmon resonance absorbance of metallic Au can be found around 500–600 nm [18–20] after thermal treatment up to 473 K. This confirms that Au deposit was not reduced through such a thermal treatment sequence, consistent

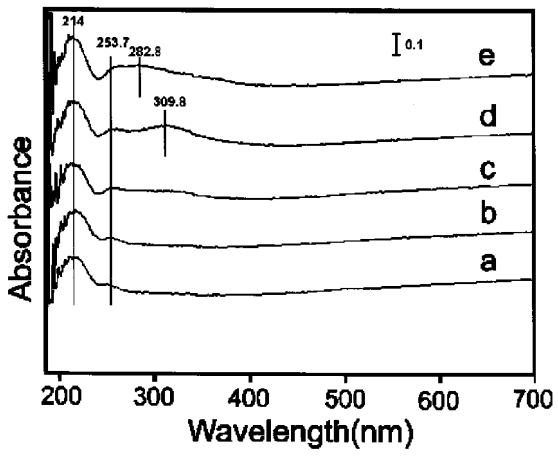

Figure 4. *In situ* diffuse-reflectance spectroscopy of the Au/γ-Al_2O_3 prepared by (a) impregnation, and that after He purge at (b) 298 K, (c) 323 K, (d) 373 K, and (e) 473 K.

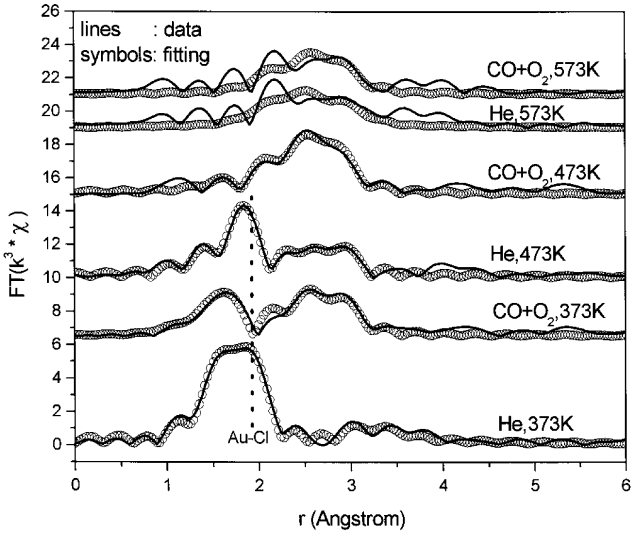

Figure 5. The radial distribution function of the Au/γ-Al_2O_3 prepared by $AuCl_3$ impregnation during CO oxidation.

with the results of EXAFS analysis. The absorbance at 214 nm is close to the ligand-to-metal charge transfer (LMCT) transition of $AuCl_3$ or $AuCl_4^-$ species observed in $Au_2Cl_{6(g)}$ [21], $AuCl_{4(aq)}^-$ [22,23], $AuCl_{3(s)}$ [24], and zeolite-supported Au catalysts [25,26]. The presence of this absorbance with all spectra in figure 4 indicates that $Au(OH)_xCl_y$ is expected to cause similar transition even when the ligand shifts. The broad absorbance bands at 254, 283, and 310 nm may be assigned to the ligand field (LF) contribution, similar to that of $AuCl_{4(aq)}^-$[22,23] reported at 286 and 322–329 nm. The same assignments over surface $AuCl_{3(s)}$ [24] and in $AuCl_3$/Na–Y [26] were reported at 320 nm and at 305 nm, respectively. Torigoe and Esumi [18] reported that an absorbance from 320–360 nm may be assigned to the interaction between $AuCl_{4(l)}^-$ and cationic surfactant. The band at 310 nm becomes more intense when the treatment temperature increased from 298 to 373 K, but it seems to be replaced by the band at 283 nm after 473 K treatment. The bands at 214 and 254 nm have higher intensity after being treated to 373 K. This may be due to the loss of Au–O–Al anchors as observed in EXAFS analyses.

Figure 5 shows the radial distribution functions from *in situ* EXAFS analysis during CO oxidation at three different temperatures; typical procedures used in microreactor studies were followed in this analysis. It should be mentioned that the EXAFS measurements were performed at reaction temperatures in this case. The Au–Cl coordination seems to disappear under 1% CO + 10% O_2 at 373 K. However, a peak close to the position of Au–Cl coordination appears again after this 373 K reaction test, i.e., under He at 473 K. This implies that 1 h CO oxidation at 373 K can remove residual chlorine, though not completely, under reaction conditions used in this study. The XANES spectra in figure 6 shows again that the catalyst was gradually reduced under CO oxidation at 373 K and above. Compared to the XANES after thermal treatment (figure 3), it suggests that the reduction of Au is mainly due to CO oxidation reactants instead of temperature.

Table 2 lists the results of detailed EXAFS analysis and the goodness of fitting can be found in figures 5 and 7. After 373 K reaction, Au–O–Al disappeared and Au-Au coordination appeared. The Au–Au coordination gradually increased with increasing reaction temperature. This indicates an increase in the degree of Au reduction and agglomeration with increasing reaction temperature. The coordination number of Au–Cl shell after 373 K CO oxidation test (table 2) is significantly lower than that after thermal treatment in He at the same temperature (table 1). However, CO oxidation at 373 K for 1 h was insufficient to remove all the chlorine because Au–Cl coordination remained in the sample at 473 K under He. Another hour of CO oxidation at

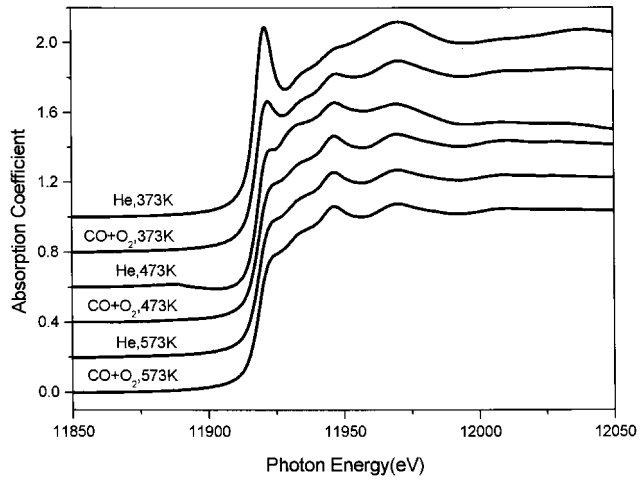

Figure 6. Au L_3-XANES of the Au/γ-Al_2O_3 prepared by $AuCl_3$ impregnation during CO oxidation.

Table 2
EXAFS analysis results of the Au/γ-Al_2O_3 prepared by impregnation during CO oxidation

Sample	Shell	r (Å)	C.N.	σ^2	E_0 (eV)	r-factor
He 373 K	Au–O	2.001±0.033	2.0±1.0	0.003±0.002	8.1±2.9	0.016
	Au–Cl	2.273±0.021	1.0±0.7	0.001±0.003		
	Au····Al	3.533±0.063	7.5±6.7	0.030±0.018		
CO oxidation 373 K	Au–O	2.005±0.012	1.8±0.4	0.007±0.002	3.7±1.6	0.041
	Au–Au	2.850±0.009	4.7±1.0	0.010±0.001		
He 473 K	Au–O	2.005[a]	1.4±0.7	0.010±0.005	1.7±1.2	0.023
	Au–Cl	2.253±0.006	0.6±0.2	0.001±0.001		
	Au–Au	2.840±0.009	3.3±1.0	0.009±0.002		
CO oxidation 473 K	Au–O	2.013±0.036	0.3±0.4	0.004±0.008	−1.2±1.7	0.029
	Au–Au	2.822±0.009	8.7±1.5	0.011±0.001		
He 573 K	Au–Au	2.841±0.027	8.4±3.8	0.014±0.003	2.2±4.3	0.313
CO oxidation 573 K	Au–Au	2.842±0.020	6.3±2.2	0.012±0.002	3.0±3.6	0.216

[a]The parameter was fixed during fitting to facilitate convergence.

473 K completely removed Cl from Au since no Au–Cl bond was observed hereafter.

The CO oxidation over the fresh sample according to a stepwise temperature-ascending–descending sequence is shown in figure 8. The catalyst gave a very high CO conversion at 573 K, but showed very low activity at temperatures below 373 K. The conversion levels were found essentially indistinguishable between the temperature ascending and descending sequences. Since *in situ* EXAFS showed that the catalyst became reduced after CO oxidation at 573 K, the extent of Au reduction is insufficient to explain the low activity at lower temperatures. In addition, the fresh sample after He purge at 473 K was also tested for CO oxidation. This was intended to compare the activity that resulted from the Au morphology containing more Cl coordination, as indicated from the *in situ* EXAFS analysis during thermal treatment. The effect of reaction temperature on CO conversions was found to be essentially the same as the fresh sample, as shown in figure 8. This suggests that the presence of Cl coordination is not the only reason responsible for the low conversion at lower reaction temperatures.

4. Discussion

It should be noted that the fresh catalyst in this study was dried at room temperature under a rough vacuum. All the above results indicate that $AuCl_3$ precursor preferred to deposit via surface –OH anchoring. The chlorine in the precursor was replaced and the chlorine residue either resided on nearby γ-Al_2O_3 surface or incorporated into the support. Such chlorine appeared to be mobile enough to make coordination to Au again when heated. A thermal treatment to 373 K caused

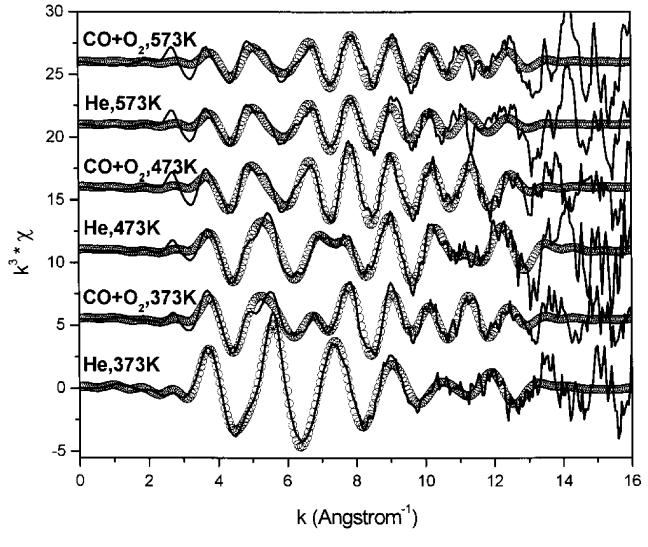

Figure 7. The k^3-weighted Chi function of the Au/γ-Al_2O_3 prepared by $AuCl_3$ impregnation during CO oxidation.

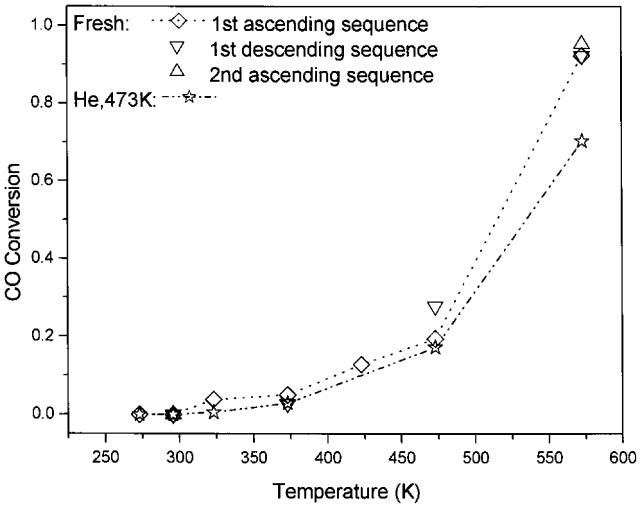

Figure 8. CO oxidations over the fresh and the 473 K treated Au/γ-Al_2O_3 prepared by $AuCl_3$ impregnation.

Au–Cl bonds to form significantly. This implies that a typical oven drying at around 373 K will cause Au deposit to contain significant amount of Cl coordination, if Cl is present in the catalyst. However, the surface Au deposit started reducing at 373 K in the presence of CO and O_2 and appeared to be removed permanently away from Au after CO oxidation at 473 K and above, under the CO oxidation conditions used in this study.

The mechanism of Au deposition observed in this study indicates a chlorine-free deposit via bonding with surface hydroxyls. Fedoseyeva and Zvonareva [14] and Nechayev and Nikolenko [15] proposed that aqueous $Au(OH)_xCl^-_{4-x}$ ions and $Au(OH)_yCl_{3-y}(H_2O)$ neutral species deposited on γ-Al_2O_3 via reacting with surface $-OH$ to have one Cl or OH ligand replaced by surface O-anchor. Lee and Gavriilidis [27] recently explained their observations of differently prepared Au/γ-Al_2O_3 catalysts and attributed the higher activity to adspecies such as $AuCl(OH)^-_3$. No chlorine-free Au adspecies was indicated in their results. Machesky *et al.* [28] proposed an adsorption scheme for $AuCl_{3(aq)}$ over goethite as: $AuCl_2(OH)(H_2O) + 2(Fe–OH^+_2) = (Fe–O–)_2Au(OH)(H_2O) + 2Cl^- + 4H^+$, where the neutral $AuCl_2(OH)(H_2O)$ was considered as the predominant aqueous species at low pH. This results in a chlorine-free Au deposit. It may be an applicable deposition mechanism for this study since the $AuCl_3$ impregnation solution used has a low pH (ca. 2–3).

One other thing that should be mentioned is the three-coordinated Au centers observed in tables 1 and 2. Au(III) species typically have a coordination number of four [29], whereas Au(I) typically have two coordinations [30]. Since reference compounds, i.e., $AuCl_3$ and $Au(OH)_3$ showed the same 3-coordinated Au centers under similar EXAFS analysis, the Au deposit is not considered to form a novel structure. The observed 3-coordinated Au species may be due to a mixture of 4-coordinated Au(III) and 2-coordinated Au(I) species. If this is true, it implies the presence of self-redox reaction in both the reference compounds and during the impregnation of $AuCl_{3(aq)}$ on γ-Al_2O_3 surface. The reference compounds are hygroscopic and became at least partially moistened during EXAFS measurements. Its self-redox in aqueous phase is puzzling but may not be impossible. Another more likely attribution of the 3-coordinated species observed in EXAFS measurement is that one of the four coordinations in Au(III) species belonged to a weak

Table 3
Different EXAFS analysis results for the Au/γ-Al_2O_3 during *in situ* CO oxidation test at 573 K

Data	*k*-range (Å^{-1})	Shell	R(Å)	C.N.	σ^2	E_0	*r*-factor
He, 573 K	3-11	Au–Au	2.813±0.017	7.4±2.2	0.013±0.002	−0.8±2.8	0.081
		Au–O	1.990±0.026	0.2±0.2	−0.003±0.007	−1.4±2.3	0.033
		Au–Au	2.810±0.014	0.6±1.6	0.012±0.002		
	3–13	Au–O	2.040[a]	0.4±0.5	0.005±0.011	−0.7±2.2	0.049
		Au–Au	2.814±0.014	6.5±1.9	0.012±0.002		
		Au–Au	2.841±0.027	8.4±3.8	0.014±0.003	2.2±4.3	0.313
		Au–O	2.083±0.023	0.003±0.01	−0.018±0.013	0.2±3.6	0.170
		Au–Au	2.827±0.025	10.5±4.3	0.016±0.003		
		Au–O	2.040[a]	0.3±0.7	0.004±0.017	1.0±4.1	0.291
		Au–Au	2.835±0.027	8.2±4.2	0.014±0.004		
$CO+O_2$, 573 K	3–11	Au–Au	2.812±0.014	6.5±1.7	0.011±0.002	−0.8±2.4	0.056
		Au–O	2.040[a]	1.2±1.1	0.018±0.013	−1.7±1.5	0.024
		Au–Au	2.807±0.009	5.1±1.2	0.010±0.002		
		Au–O	2.040[a]	0.6±0.8	0.011±0.014		
		Au–Au	2.828±0.023	7.8±3.1	0.013±0.004	−0.3±2.8	0.017
		Au–(O)–Au	3.113±0.043	0.5±1.8	0.003±0.021		
	3–13	Au–O	2.071±0.127	1.0±2.5	0.017±0.003		
		Au–Au	2.830±0.032	7.0±6.1	0.012±0.010	0.4±6.5	0.016
		Au–(O)–Au	3.108±0.111	0.5±3.3	0.004±0.043		
		Au–Au	2.842±0.020	6.3±2.2	0.012±0.002	3.0±3.6	0.216
		Au–O	2.040[a]	0.4±0.8	0.007±0.002	1.7±3.4	0.196
		Au–Au	2.837±0.019	6.4±2.5	0.012±0.002		
		Au–O	2.077±0.022	0.006±0.02	−0.016±0.009		
		Au–Au	2.844±0.035	13.0±4.8	0.018±0.003	1.0±4.3	0.053
		Au–(O)–Au	3.152±0.021	2.2±3.6	0.010±0.009		
		Au–O	2.040[a]	0.3±0.9	0.006±0.003		
		Au–Au	2.849±0.030	6.7±6.1	0.012±0.005	4.7±7.3	0.183
Au–(O)–Au		3.147±0.181	16.6±111	0.047±0.158			

[a]The parameter was fixed during fitting to facilitate convergence.

coordination that causes insignificant EXAFS backscattered signal. If moisture acts as such weak coordination, an adspecies like

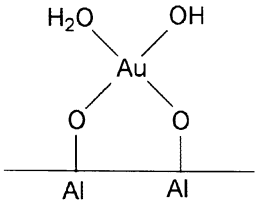

serves as a possible morphology, which is consistent with the proposed deposition mechanism from $AuCl_2(OH)(H_2O)$ as discussed above. Hydrated Au oxyhydroxide ($AuOOH.xH_2O$) proposed in Au–Fe coprecipitated catalysts [31] and in TiO_2-modified $Au(OH)_3$ [32,33] may be another possible morphology.

Figure 8 shows that the catalyst can achieve almost 100% CO conversion at 573 K. This seems to indicate that the removal of chlorine and the reduction of Au caused the activity enhancement. However, this is not considered true. It is because that no activity enhancement was observed during the temperature-descending sequence in the test, i.e., after the catalyst reached 573 K. One may suspect that Au particle sintering may remedy the presumed activity enhancement. However, the Au–Au coordination number after CO oxidation at 573 K (table 2) indicates insignificant sintering effect. This clearly shows that neither the chlorine residue nor the extent of Au reduction can be considered as the main reason for the low activity at temperatures below 373 K.

It should be pointed out that the EXAFS fitting to the data at 573 K in the *in situ* CO oxidation test (figure 5) seem unsatisfactory. All other model fittings reported in this study showed satisfactory match to original data. This makes it ambiguous to use the EXAFS analysis results to interpret the enhanced activity at 573 K. From the r-space spectra shown in figure 5, bands appear at 1.7 and 2.2 Å (without phase correction) for the data taken at 573 K. The presence of the 2.2 Å peak seems to cause the fitting Au–Au shell to shift to shorter bond distance, as shown in figure 5 and table 2. If the Au–Au bond distance were fixed at standard value, the fitting would result in a smaller Au–Au coordination number; nothing else was significantly altered. This 2.2 Å peak seems to coincide with an assigned short Au–Au metallic coordination at 2.4 Å, reported by Cunningham *et al.* [34] However, this attribution is too short for Au metallic bond distance when compared to theoretical bond distances of Au clusters [35]. Okumura *et al.* [36] found a Au_x–O coordination at 2.45 Å from density functional calculation. This was included in our fitting but was unsuccessful. Au–Al alloy can be found in the literatures [37], but its presence in the fitting model was also denied. A model containing Au–O and Au-Au resulted in somewhat improved fitting with those data taken at 573 K. The inclusion of a Au–(O)–Au shell further improved the fitting for the data under CO

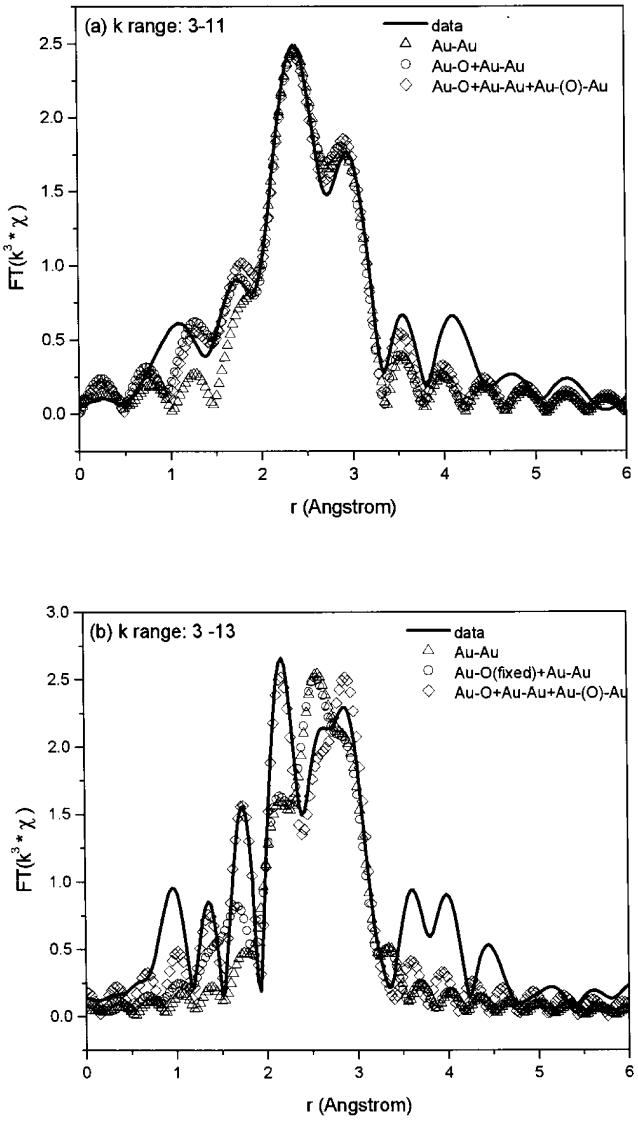

Figure 9. Comparison of EXAFS analysis results for the Au/γ-Al_2O_3 during *in situ* CO oxidation test at 573 K using a *k*-range of (a) 3–11, and (b) 3–13 $Å^{-1}$.

reaction. This suggests the presence of adsorbed oxygen, although a much-improved data quality and analysis is needed for confirmation. These fitting results using two *k*-ranges 3–11 and 3–13 $Å^{-1}$ are summarized in table 3 and figure 9. That the shape of the peak at 2.2 Å alters significantly because of the change in the k-range of data fitting suggests its origin from second shell(s).

Acknowledgments

This research is supported by National Science Council, Taiwan, R.O.C. under contract numbers NSC86-2214-E-155-005 and NSC86-2113-M-155-001. The authors also like to thank one of the referees for pointing out the possibility of the incorporation of Cl residue into the support.

References

[1] M. Haruta, S. Tsubota, T. Kobayashi, H. Kageyama, M.J. Genet and B.J. Delmon, J. Catal. 175 (1993) 144.
[2] M. Haruta, Catal. Survey Jpn. 61 (1997) 1.
[3] S. Tsubota, D.A.H. Cunningham, Y. Bando and M. Haruta, in *Preparation of Catalysts VI*, G. Poncelet (ed.), *et al.* (Elsevier, Amsterdam, 1995) p. 227.
[4] M. Okumura, S. Nakamura, S. Tsubota, T. Nakamura, M. Azuma and M. Haruta, Catal. Lett. 51 (1998) 53.
[5] G.C. Bond and D.T. Thompson, Catal. Rev.-Sci. Eng. 319 (1999) 41.
[6] H.-S. Oh, J.H. Yang, C.K. Costello, Y.M. Wang, S.R. Bare, H.H. Kung and M.C. Kung, J. Catal. 210 (2002) 375.
[7] M.M. Schubert, S. Hackenberg, A.C. van Veen, M. Muhler, V. Plzak and R.J. Behm, J. Catal. 113 (2001) 197.
[8] M. Newville, B. Ravel, D. Haskel, J.J. Rehr, E.A. Stern and Y. Yacoby, Physica B 208-9 (1995) 154.
[9] A. Ankndinow, Ph.D. Thesis (University of Washington, Washington, 1996).
[10] P.G. Jones, H. Rumpel, E. Schwarzmann and G.M. Sheldrick, Acta Crystallogr. B 35 (1979) 1435.
[11] T.M. Salama, T. Shido, R. Ohnishi and M. Ichikawa, J. Phys. Chem. 100 (1996) 3688.
[12] F.W.H. Kampers, T.M.J. Maas, J. van Grondelle, P. Brinkgreve and D.C. Koningsburger, Rev. Sci. Instrum. 60 (1989) 2635.
[13] T. Yokoyama, Y. Matsukado, A. Uchida, Y. Motomura, K. Watanabe and E. Izawa, J. Colloid Interface Sci. 233 (2001) 112.
[14] V.I. Fedoseyeva and G.V. Zvonareva, Geochem. Intl. 25 (1988) 115.
[15] Y.A. Nechayev and N.V. Nikolenko, Geochem. Intl. 23 (1986) 32.
[16] C.-H. Lin, S.-H. Hsu, M.-Y. Lee and S.D. Lin, J. Catal. 209 (2002) 62.
[17] F. Farges, J.A. Sharps and G.E. Brown Jr., Geochim. Cosmochim. Acta. 57 (1993) 1243.
[18] K. Torigoe and K. Esumi, Langmuir 8 (1992) 59.
[19] D.G. Duff and A. Baiker, in *Preparation of Catalysts VI* G. Poncelet, *et al.* (eds) (Elsevier, Amsterdam, 1995) p. 505.
[20] G. Schmid, R. Pfeil, R. Boese, F. Bandermann, S. Meyer, G.H.M. Calis and W.A. Velden, Chem. Ber. 114 (1981) 3634.
[21] D.S. Rustad and N.W. Gregory, Polyhedron 10 (1991) 633.
[22] W.R. Mason and H.B. Gray, Inorg. Chem. 7 (1968) 55.
[23] A.K. Gangopadhayay and A.J. Chkravorty, J. Chem. Phys. 35 (1961) 2206.
[24] E.S. Clark and D.H. Templeton, Acta Crystallogr. 11 (1958) 284.
[25] Y.M. Kang and B.Z. Wan, Appl. Catal. A: Gen. 26 (1995) 59.
[26] T.M. Salama, T. Shido, R. Ohnishi and M. Ichikawa, J. Phys. Chem. 100 (1996) 3688.
[27] S.-J. Lee. and A. Gavriilidis, J. Catal. 206 (2002) 305.
[28] M. Machesky, W.O. Andrade and A. Rose, Geochim. Cosmochim. Acta. 55 (1991) 769.
[29] G. Cocco, S. Enzo, G. Fagherazzi, L. Schiffini, I.W. Bassi, G. Vlaic, S. Galvagno and G. Parravano, J. Phys. Chem. 83 (1979) 2527.
[30] R.J. Puddephatt, *The Chemistry of Gold*, 2nd ed. (Elsevier, 1980).
[31] R.M. Finch, N.A. Hodge, G.J. Hutchings, A. Meagher, Q.A. Pankhurst, M.R.H. Siddiqui, F.E. Wagner and R. Whyman, Phys. Chem. Chem. Phys. 1 (1999) 485.
[32] E.E. Stangland, K.B. Stavens, R.P. Andres and W.N. Delgass, in *Studies in Surface Science and Catalysis*, A. Corma, F.V. Melo, S. Mendioroz and J.L.G. Fierro (eds), Vol. 130 (Elsevier, 2000) p. 827.
[33] E.E. Stangland, K.B. Stavens, R.P. Andres and W.N. Delgass, J. Catal. 191 (2000) 332.
[34] D.A.H. Cunningham, W. Vogel, H. Kageyama, S. Tsubota and M. Haruta, J. Catal. 177 (1998) 1.
[35] G. D'Agostino, A. Pinto and S. Mobilio, Phys. Rev. B 48 (1993) 14447.
[36] M. Okumura, Y. Kitagawa, M. Haruta and K. Yamaguchi, Chem. Phys. Lett. 346 (2001) 163.
[37] H. Piao, N.S. McIntyre, G. Beamson, M.-L. Abel and J.F. Watts, J. Electron Spectrosc. Relat. Phenom. 125 (2002) 35.